A simplified model of heavy vector singlets at the FCC-hh

Based on arXiv: 2407.11117

Michael J. Baker[a], Timothy Martonhelyi[a], Andrea Thamm[a], Riccardo Torre[b]
[a] The University of Massachusetts Amherst, [b] INFN Genova

Timothy Martonhelyi,
University of Massachusetts Amherst

A simplified model of heavy vector singlets

Introduce two new vectors that transform under the SM gauge group as colourless $SU(2)_L$ singlets:

$$V^0 \sim (\mathbf{1}, \mathbf{1}, 0) \qquad \mathcal{L}_{V^0} \supset i\frac{g_V}{2} c_H^0 V_\mu^0 H^\dagger \overleftrightarrow{D}^\mu H + \frac{g_V}{2} c_\Psi^0 V_\mu^0 J_\Psi^\mu$$

$$V^\pm \sim (\mathbf{1}, \mathbf{1}, \pm 1) \qquad \mathcal{L}_{V^+} \supset i\frac{g_V}{\sqrt{2}} c_H^+ V_\mu^+ H^\dagger \overleftrightarrow{D}^\mu \tilde{H} + \frac{g_V}{\sqrt{2}} c_q^+ V_\mu^+ J_q^\mu$$

- $c_H^{0,+}$ – controls VBF and di-boson final states
- c_Ψ^0 – controls DY and neutral di-fermion decay, Ψ = {Q,L,U,D,E}
- c_q^+ – controls DY and charged di-jet final states

A simplified model of heavy vector singlets

Introduce two new vectors that transform under the SM gauge group as colourless $SU(2)_L$ singlets:

$$V^0 \sim (\mathbf{1},\mathbf{1},0) \qquad \mathcal{L}_{V^0} \supset i\frac{g_V}{2}c_H^0 V_\mu^0 H^\dagger \overleftrightarrow{D}^\mu H + \frac{g_V}{2}c_\Psi^0 V_\mu^0 J_\Psi^\mu$$

$$V^\pm \sim (\mathbf{1},\mathbf{1},\pm 1) \qquad \mathcal{L}_{V^+} \supset i\frac{g_V}{\sqrt{2}}c_H^+ V_\mu^+ H^\dagger \overleftrightarrow{D}^\mu \tilde{H} + \frac{g_V}{\sqrt{2}}c_q^+ V_\mu^+ J_q^\mu$$

- $c_H^{0,+}$ – controls VBF and di-boson final states
- c_Ψ^0 – controls DY and neutral di-fermion decay, Ψ = {Q,L,U,D,E}
- c_q^+ – controls DY and charged di-jet final states

Under the narrow width approximation, the combinations $g_V c_X$ parameterise decay rates and cross sections:

$$\sigma \times \mathrm{BR} \propto (g_V c_X)^2 \times (g_V c_Y)^2$$

A simplified model of heavy vector singlets

Introduce two new vectors that transform under the SM gauge group as colourless $SU(2)_L$ singlets:

$$V^0 \sim (\mathbf{1},\mathbf{1},0) \qquad \mathcal{L}_{V^0} \supset i\frac{g_V}{2}c_H^0 V_\mu^0 H^\dagger \overleftrightarrow{D}^\mu H + \frac{g_V}{2}c_\Psi^0 V_\mu^0 J_\Psi^\mu$$

$$V^\pm \sim (\mathbf{1},\mathbf{1},\pm 1) \qquad \mathcal{L}_{V^+} \supset i\frac{g_V}{\sqrt{2}}c_H^+ V_\mu^+ H^\dagger \overleftrightarrow{D}^\mu \tilde{H} + \frac{g_V}{\sqrt{2}}c_q^+ V_\mu^+ J_q^\mu$$

- $c_H^{0,+}$ – controls VBF and di-boson final states
- c_Ψ^0 – controls DY and neutral di-fermion decay, Ψ = {Q,L,U,D,E}
- c_q^+ – controls DY and charged di-jet final states

Under the narrow width approximation, the combinations $g_V c_X$ parameterise decay rates and cross sections:

$$\sigma \times \mathrm{BR} \propto (g_V c_X)^2 \times (g_V c_Y)^2$$

A simplified model of heavy vector singlets

Introduce two new vectors that transform under the SM gauge group as colourless $SU(2)_L$ singlets:

$$V^0 \sim (\mathbf{1},\mathbf{1},0) \qquad \mathcal{L}_{V^0} \supset i\frac{g_V}{2} c_H^0 V_\mu^0 H^\dagger \overleftrightarrow{D}^\mu H + \frac{g_V}{2} c_\Psi^0 V_\mu^0 J_\Psi^\mu$$

$$V^\pm \sim (\mathbf{1},\mathbf{1},\pm 1) \qquad \mathcal{L}_{V^+} \supset i\frac{g_V}{\sqrt{2}} c_H^+ V_\mu^+ H^\dagger \overleftrightarrow{D}^\mu \tilde{H} + \frac{g_V}{\sqrt{2}} c_q^+ V_\mu^+ J_q^\mu$$

- $c_H^{0,+}$ – controls VBF and di-boson final states
- c_Ψ^0 – controls DY and neutral di-fermion decay, Ψ = {Q,L,U,D,E}
- c_q^+ – controls DY and charged di-jet final states

Under the narrow width approximation, the combinations $g_V c_X$ parameterise decay rates and cross sections:

$$\sigma \times \mathrm{BR} \propto (g_V c_X)^2 \times (g_V c_Y)^2$$

Production and decay

We consider Drell-Yan production of the heavy vector and decay to two-body final states. Use the benchmark $c_X^0 = 1$ to get a rough sense of production and decay rates:

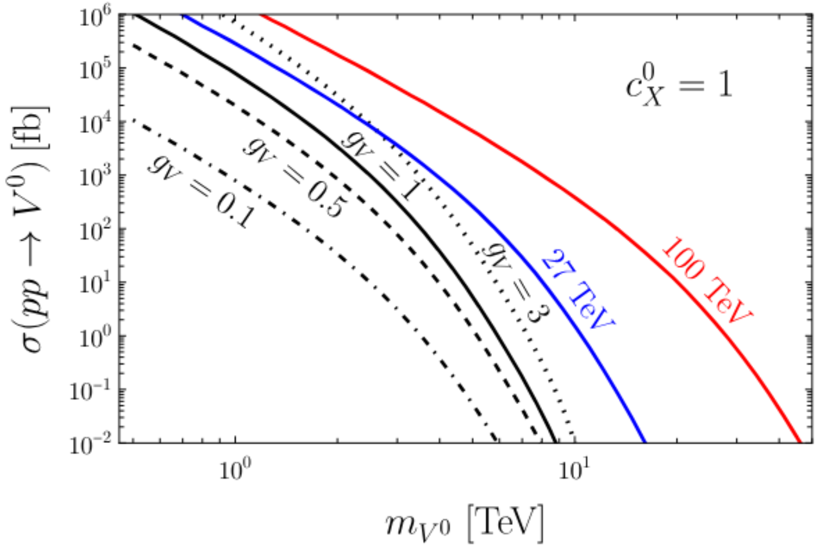

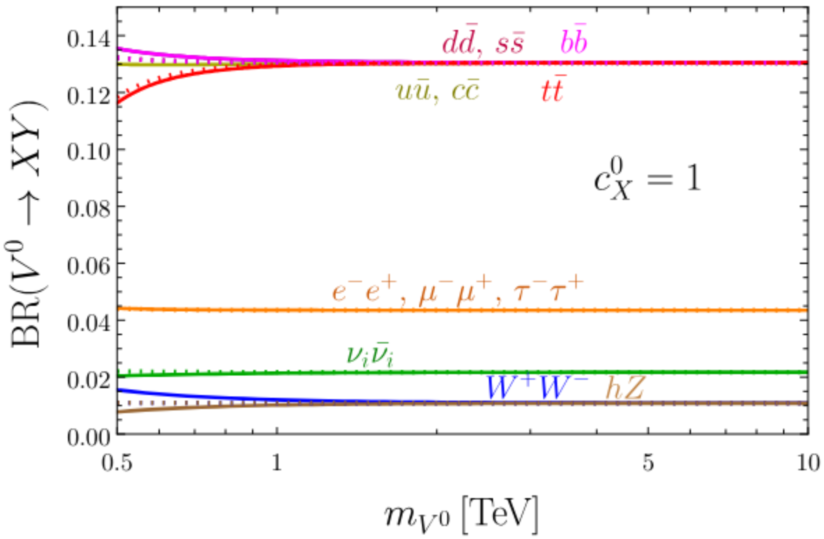

Simplified models

Simplified models provide a phenomenological bridge between the wide variety of BSM theories and experimental searches:

Simplified models

Simplified models provide a phenomenological bridge between the wide variety of BSM theories and experimental searches:

Straightforwardly obtain cross-section limits for explicit models

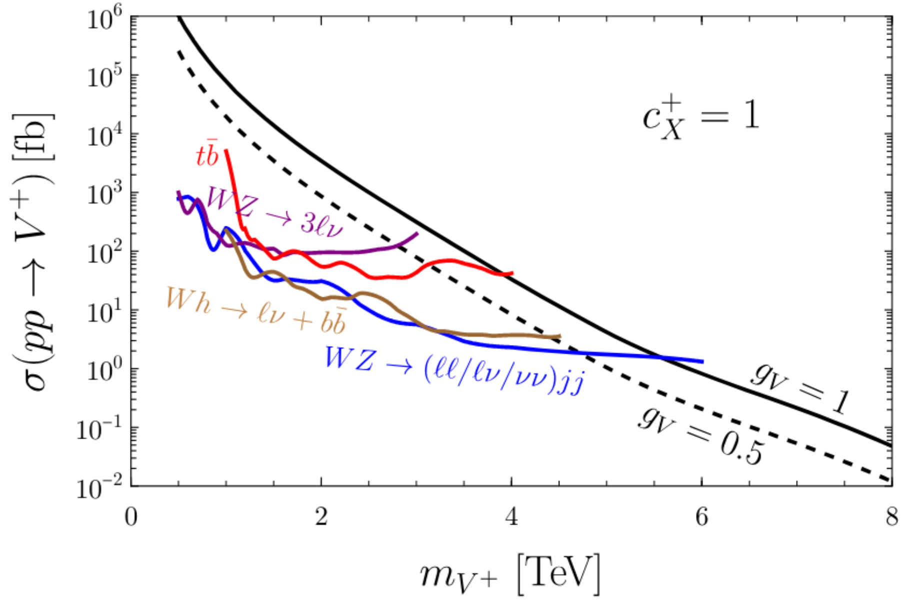

Simplified models

Simplified models provide a phenomenological bridge between the wide variety of BSM theories and experimental searches:

Straightforwardly obtain cross-section limits for explicit models

Model-independent limits on the parameter space can easily be compared to limits on explicit models

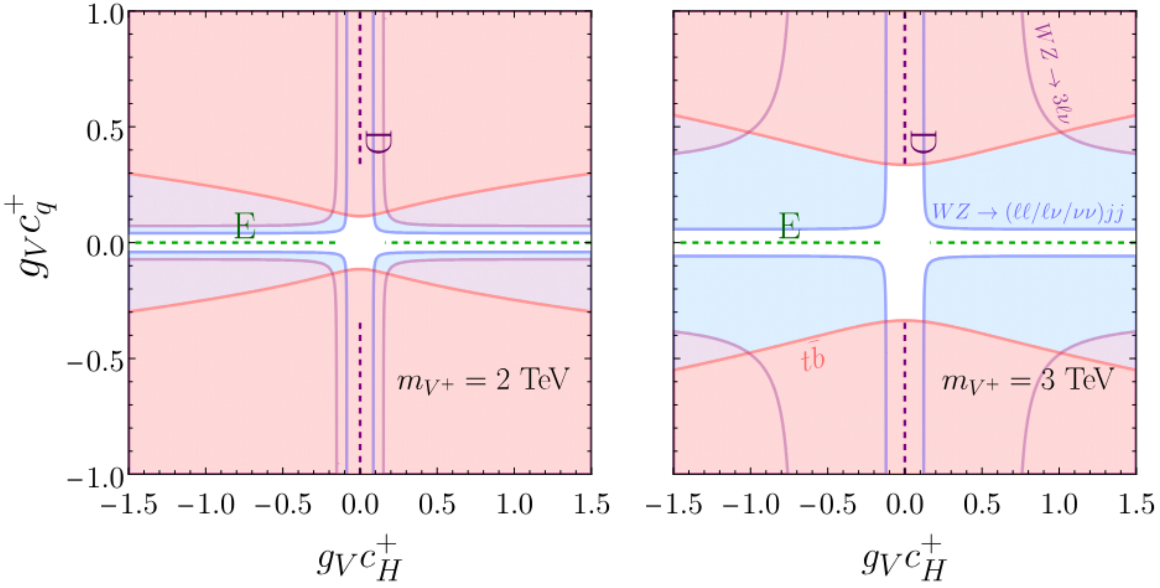

Simplified models

Simplified models provide a phenomenological bridge between the wide variety of BSM theories and experimental searches:

Straightforwardly obtain cross-section limits for explicit models

Model-independent limits on the parameter space can easily be compared to limits on explicit models

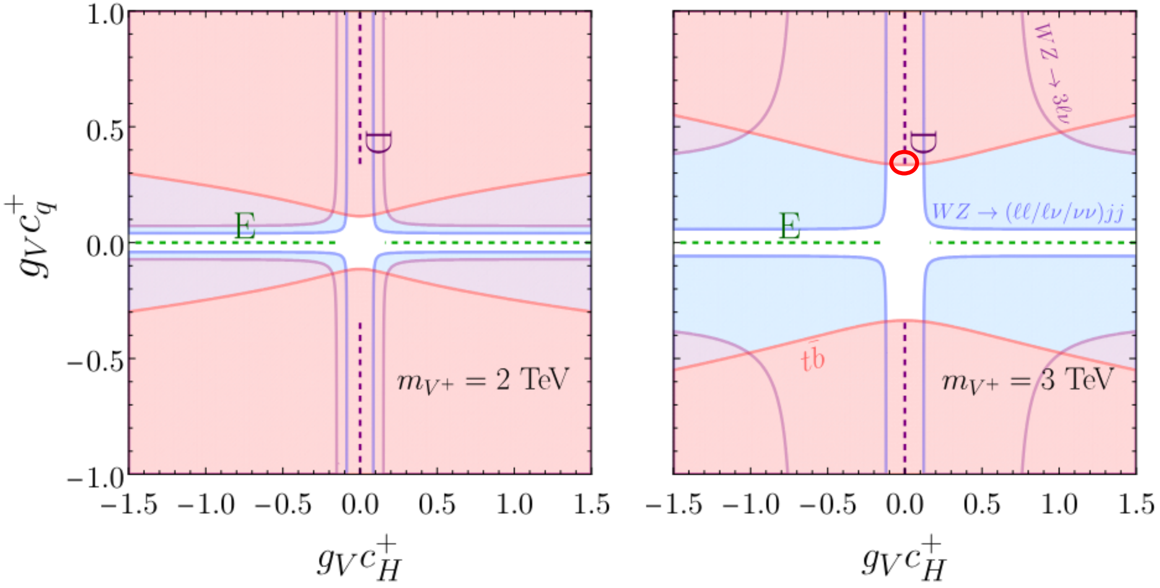

Simplified models

Simplified models provide a phenomenological bridge between the wide variety of BSM theories and experimental searches:

Straightforwardly obtain cross-section limits for explicit models

Model-independent limits on the parameter space can easily be compared to limits on explicit models

For more model-dependent analysis, convert into limits in the mass-coupling plane

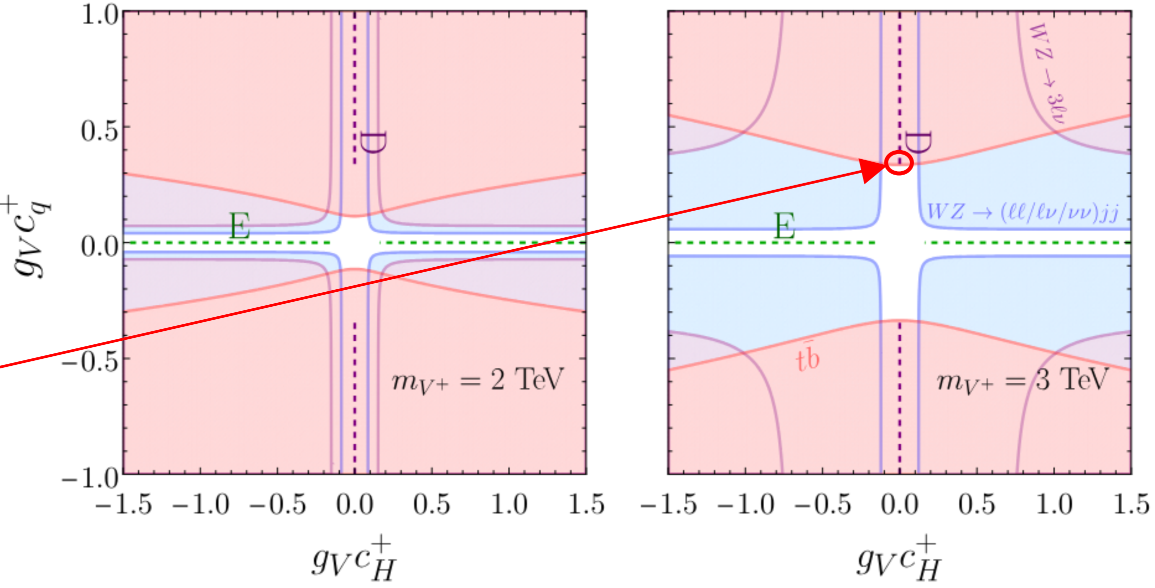

Simplified models

Simplified models provide a phenomenological bridge between the wide variety of BSM theories and experimental searches:

Straightforwardly obtain cross-section limits for explicit models

Model-independent limits on the parameter space can easily be compared to limits on explicit models

For more model-dependent analysis, convert into limits in the mass-coupling plane

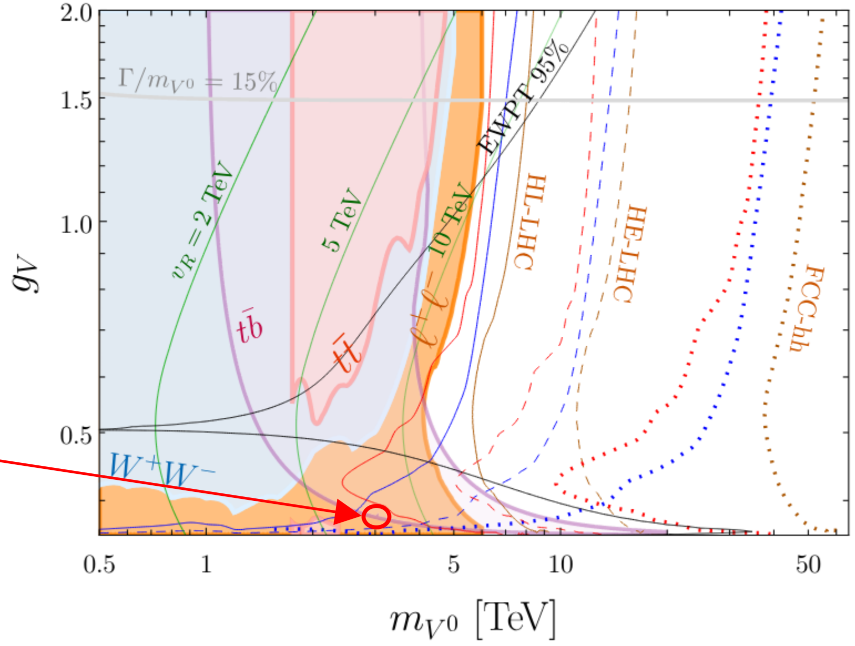

Extrapolating LHC limits to future colliders

We can take limits obtained at the LHC and project to future colliders of CoM energy √s and luminosity √L. The upper limit on the number of signal events is driven by the background in a window surrounding the resonance mass.
For the FCC-hh, we take:

√s = 100 TeV
√L = 20 ab^{-1}

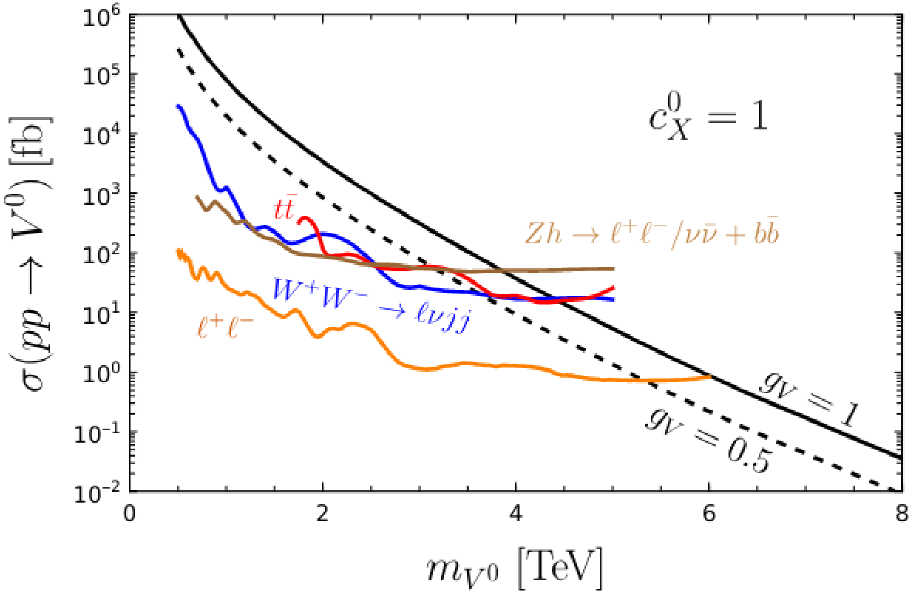

Extrapolating LHC limits to future colliders

We can take limits obtained at the LHC and project to future colliders of CoM energy √s and luminosity √L. The upper limit on the number of signal events is driven by the background in a window surrounding the resonance mass.
For the FCC-hh, we take:

√s = 100 TeV
√L = 20 ab^{-1}

Equating backgrounds of two colliders:

$$B(s_0, L_0, m_0) = B(s, L, m)$$

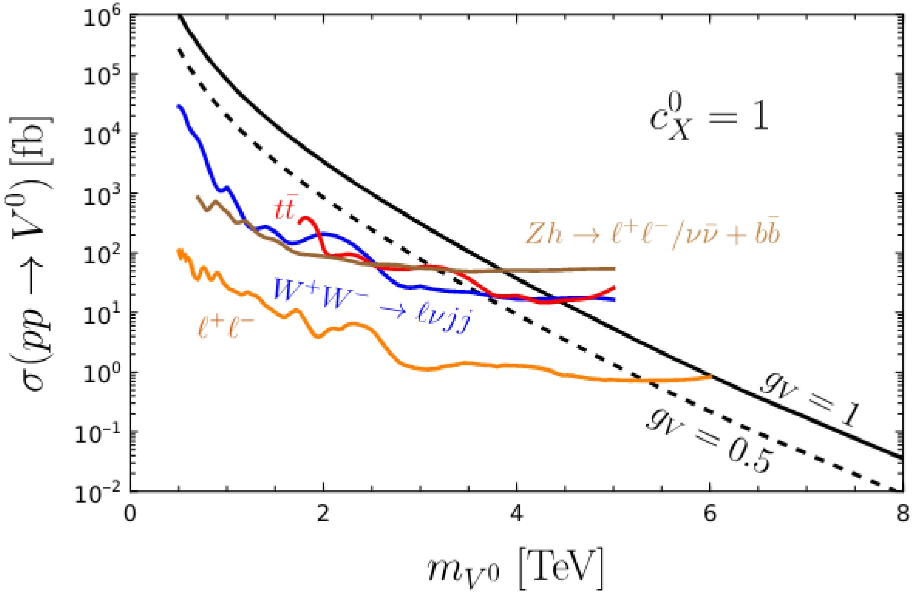

Extrapolating LHC limits to future colliders

We can take limits obtained at the LHC and project to future colliders of CoM energy √s and luminosity √L. The upper limit on the number of signal events is driven by the background in a window surrounding the resonance mass.
For the FCC-hh, we take:

√s = 100 TeV
√L = 20 ab^{-1}

Equating backgrounds of two colliders:

$$B(s_0, L_0, m_0) = B(s, L, m)$$

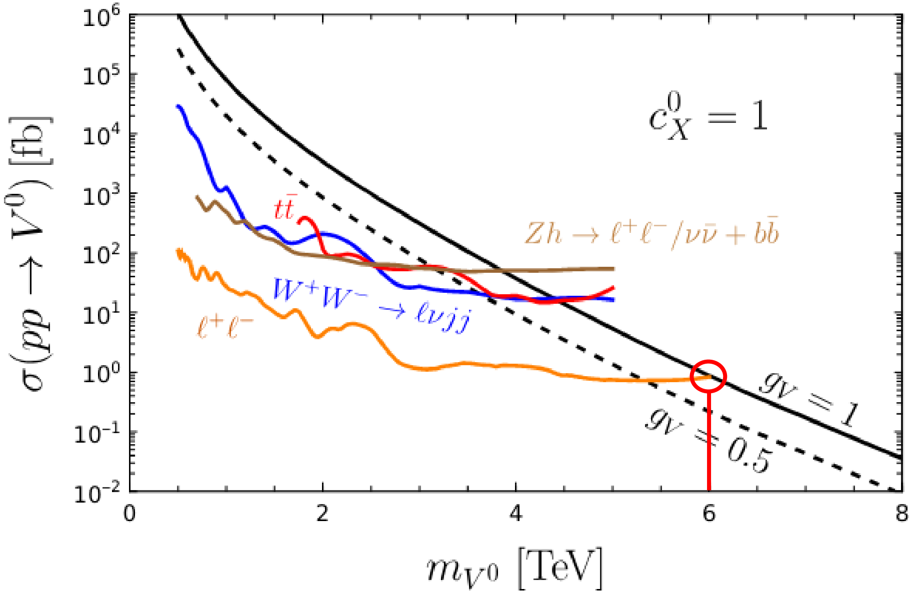

Extrapolating LHC limits to future colliders

We can take limits obtained at the LHC and project to future colliders of CoM energy √s and luminosity √L. The upper limit on the number of signal events is driven by the background in a window surrounding the resonance mass.
For the FCC-hh, we take:

√s = 100 TeV
√L = 20 ab^{-1}

Equating backgrounds of two colliders:

$$B(s_0, L_0, m_0) = B(s, L, m)$$

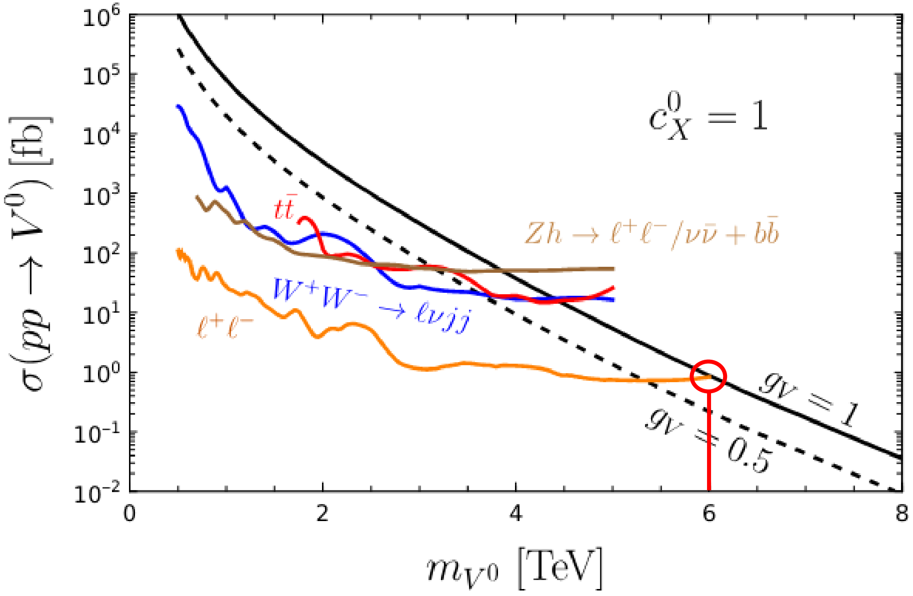

Extrapolating LHC limits to future colliders

We can take limits obtained at the LHC and project to future colliders of CoM energy √s and luminosity √L. The upper limit on the number of signal events is driven by the background in a window surrounding the resonance mass.
For the FCC-hh, we take:

√s = 100 TeV

√L = 20 ab^{-1}

Equating backgrounds of two colliders:

$$B(s_0, L_0, m_0) = B(s, L, m)$$

$$\sum_{\{i,j\}} c_{ij} \frac{d\mathcal{L}_{ij}}{d\hat{s}}(m; \sqrt{s}) = \frac{L_0}{L} \sum_{\{i,j\}} c_{ij} \frac{d\mathcal{L}_{ij}}{d\hat{s}}(m_0; \sqrt{s_0})$$

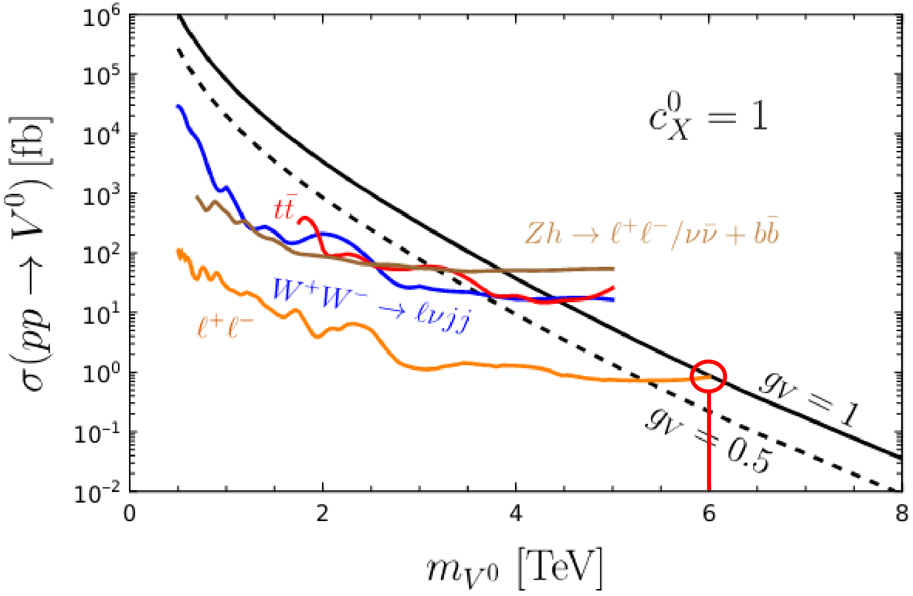

Extrapolating LHC limits to future colliders

We can take limits obtained at the LHC and project to future colliders of CoM energy √s and luminosity √L. The upper limit on the number of signal events is driven by the background in a window surrounding the resonance mass.
For the FCC-hh, we take:

√s = 100 TeV
√L = 20 ab^{-1}

Equating backgrounds of two colliders:

$$B(s_0, L_0, m_0) = B(s, L, m)$$

$$\sum_{\{i,j\}} c_{ij} \frac{d\mathcal{L}_{ij}}{d\hat{s}}(m; \sqrt{s}) = \frac{L_0}{L} \sum_{\{i,j\}} c_{ij} \frac{d\mathcal{L}_{ij}}{d\hat{s}}(m_0; \sqrt{s_0})$$

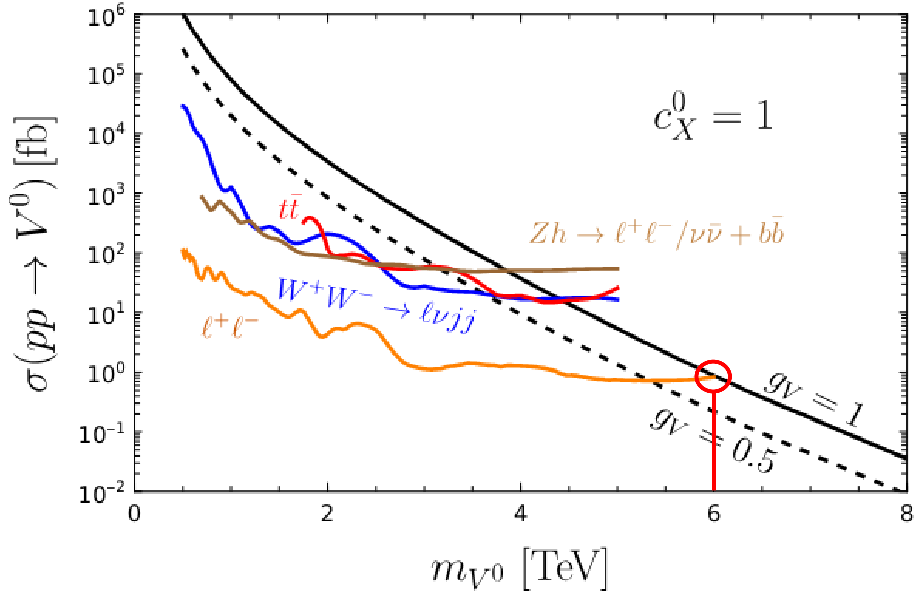

Extrapolating LHC limits to future colliders

We can take limits obtained at the LHC and project to future colliders of CoM energy √s and luminosity √L. The upper limit on the number of signal events is driven by the background in a window surrounding the resonance mass.
For the FCC-hh, we take:

√s = 100 TeV

√L = 20 ab^{-1}

Equating backgrounds of two colliders:

$$B(s_0, L_0, m_0) = B(s, L, m)$$

$$\sum_{\{i,j\}} c_{ij} \frac{d\mathcal{L}_{ij}}{d\hat{s}}(m; \sqrt{s}) = \frac{L_0}{L} \sum_{\{i,j\}} c_{ij} \frac{d\mathcal{L}_{ij}}{d\hat{s}}(m_0; \sqrt{s_0})$$

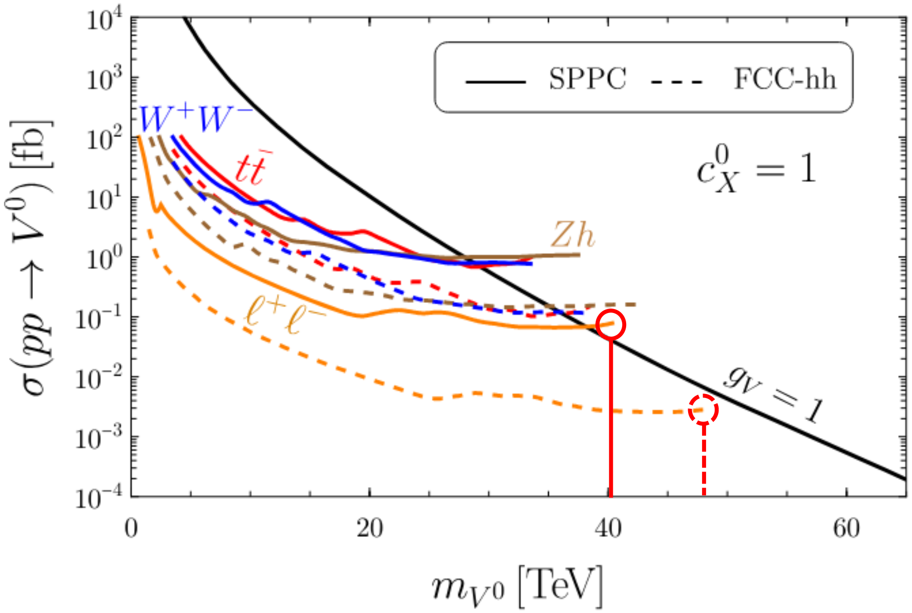

Extrapolating LHC limits to future colliders

We can take limits obtained at the LHC and project to future colliders of CoM energy √s and luminosity √L. The upper limit on the number of signal events is driven by the background in a window surrounding the resonance mass.
For the FCC-hh, we take:

√s = 100 TeV

√L = 20 ab^{-1}

Equating backgrounds of two colliders:

$$B(s_0, L_0, m_0) = B(s, L, m)$$

$$\sum_{\{i,j\}} c_{ij} \frac{d\mathcal{L}_{ij}}{d\hat{s}}(m; \sqrt{s}) = \frac{L_0}{L} \sum_{\{i,j\}} c_{ij} \frac{d\mathcal{L}_{ij}}{d\hat{s}}(m_0; \sqrt{s_0})$$

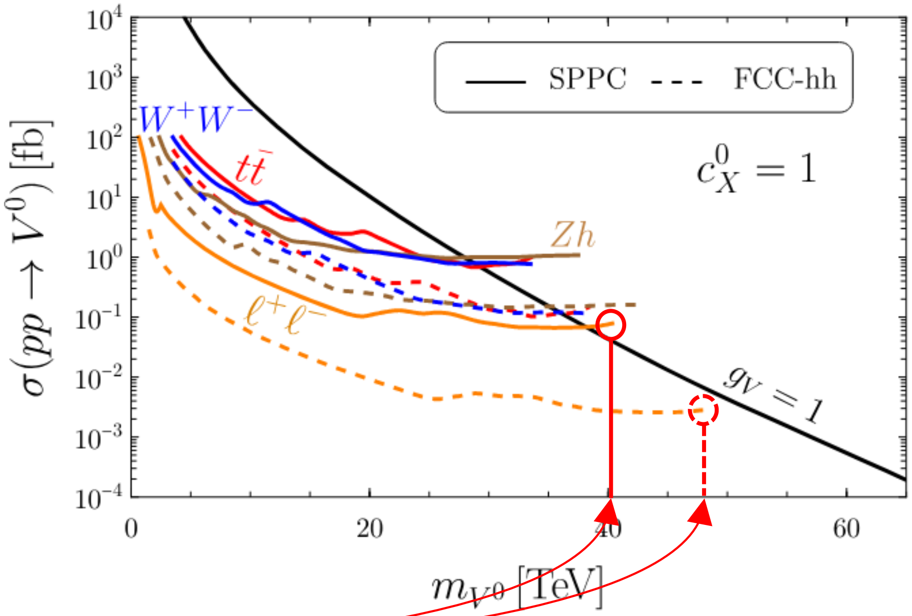

Extrapolating LHC limits to future colliders

We can take limits obtained at the LHC and project to future colliders of CoM energy √s and luminosity √L. The upper limit on the number of signal events is driven by the background in a window surrounding the resonance mass.
For the FCC-hh, we take:

√s = 100 TeV

√L = 20 ab^{-1}

FCC-hh best positioned to explore the multi-TeV region

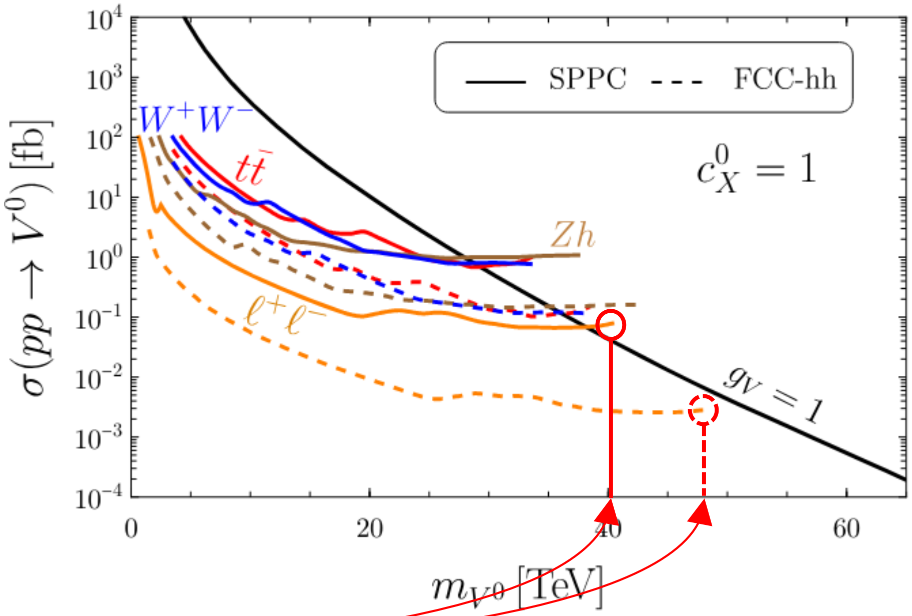

Equating backgrounds of two colliders:

$$B(s_0, L_0, m_0) = B(s, L, m)$$

$$\sum_{\{i,j\}} c_{ij} \frac{d\mathcal{L}_{ij}}{d\hat{s}}(m; \sqrt{s}) = \frac{L_0}{L} \sum_{\{i,j\}} c_{ij} \frac{d\mathcal{L}_{ij}}{d\hat{s}}(m_0; \sqrt{s_0})$$

Electroweak precision tests

Under the heavy vector singlet model, the oblique parameters get the following contributions at leading order in m_W^2/m_V^2:

$$\hat{S} \equiv \frac{\alpha(m_Z)}{4\sin^2\theta_W} S = \frac{g_V^2 m_W^2}{2g^2 g'^2 m_{V^0}^2}(c_E^0 - c_H^0 + c_L^0)(g^2 c_E^0 + g'^2(c_E^0 + 2c_L^0))$$

$$\hat{T} \equiv \alpha(m_Z) T = \frac{g_V^2 m_W^2}{g^2 m_{V^0}^2}(c_E^0 - c_H^0 + c_L^0)^2 - \frac{g_V^2 (c_H^+)^2 m_W^2}{g^2 m_{V^+}^2}$$

$$\hat{U} \equiv -\frac{\alpha(m_Z)}{4\sin^2\theta_W} U = \frac{g_V^2 m_W^2}{g^2 m_{V^0}^2}(c_E^0 - c_H^0 + c_L^0)(c_E^0 + 2c_L^0)$$

	Result	S	T	U
S	-0.04 ± 0.1	1	0.93	-0.7
T	0.01 ± 0.12		1	-0.87
U	-0.01 ± 0.09			1

Values from 2024 PDG

	FCCee							
	Z (no pol)		Z (pol)		WW		$t\bar{t}$	
ΔS $[\times 10^{-3}]$	12	7.8	11	6.4	11	6.4	11	6.3
ΔT $[\times 10^{-3}]$	13	8.1	13	7.9	13	7.9	12	5.8
ΔU $[\times 10^{-3}]$	32	31	32	31	9.8	5.4	9.6	5.2

1608.01509: J. de Blas, M. Ciuchini, E. Franco, S. Mishima, M. Pierini, L. Reina, L. Silvestrini

Electroweak precision tests

Under the heavy vector singlet model, the oblique parameters get the following contributions at leading order in m_W^2/m_V^2:

$$\hat{S} \equiv \frac{\alpha(m_Z)}{4\sin^2\theta_W} S = \frac{g_V^2 m_W^2}{2g^2 g'^2 m_{V^0}^2}(c_E^0 - c_H^0 + c_L^0)(g^2 c_E^0 + g'^2(c_E^0 + 2c_L^0))$$

$$\hat{T} \equiv \alpha(m_Z) T = \frac{g_V^2 m_W^2}{g^2 m_{V^0}^2}(c_E^0 - c_H^0 + c_L^0)^2 - \frac{g_V^2 (c_H^+)^2 m_W^2}{g^2 m_{V^+}^2}$$

$$\hat{U} \equiv -\frac{\alpha(m_Z)}{4\sin^2\theta_W} U = \frac{g_V^2 m_W^2}{g^2 m_{V^0}^2}(c_E^0 - c_H^0 + c_L^0)(c_E^0 + 2c_L^0)$$

	Result	S	T	U
S	-0.04 ± 0.1	1	0.93	-0.7
T	0.01 ± 0.12		1	-0.87
U	-0.01 ± 0.09			1

Values from 2024 PDG

	FCCee							
	Z (no pol)		Z (pol)		WW		$t\bar{t}$	
ΔS $[\times 10^{-3}]$	12	7.8	11	6.4	11	6.4	11	6.3
ΔT $[\times 10^{-3}]$	13	8.1	13	7.9	13	7.9	12	5.8
ΔU $[\times 10^{-3}]$	32	31	32	31	9.8	5.4	9.6	5.2

1608.01509: J. de Blas, M. Ciuchini, E. Franco, S. Mishima, M. Pierini, L. Reina, L. Silvestrini

Comparing limits for explicit models

Model:

$U(1)_{B-L}$ gauge symmetry

- Approx. 5 TeV mass reach at LHC, 40–50 TeV at FCC-hh
- EWPTs are better for most couplings, except very small g_V
- FCC-hh will reach all those regions covered by EWPTs, as well as small couplings

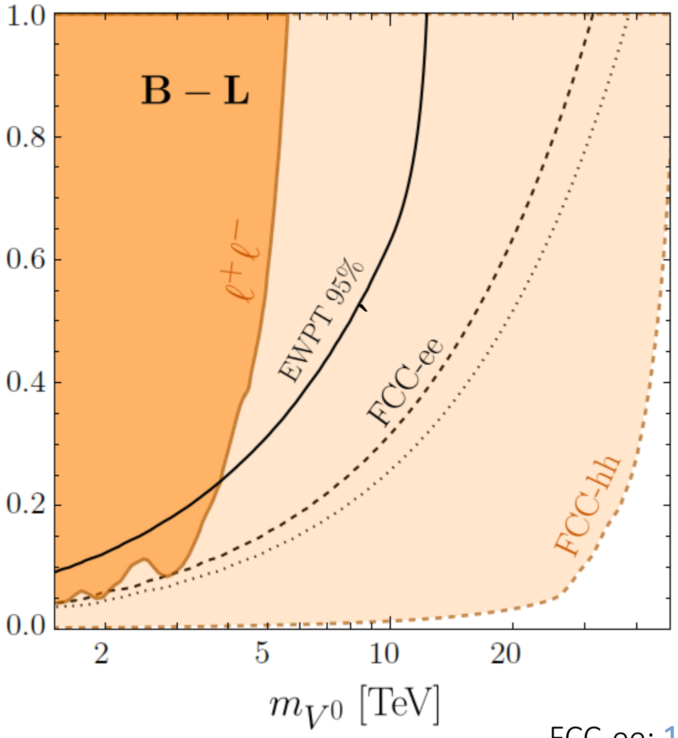

FCC-ee: 1608.01509

Comparing limits for explicit models

Model: $SU(2)_R \times U(1)_X$

Left-right gauge symmetry (weakly coupled)

FCC-ee: [1608.01509]

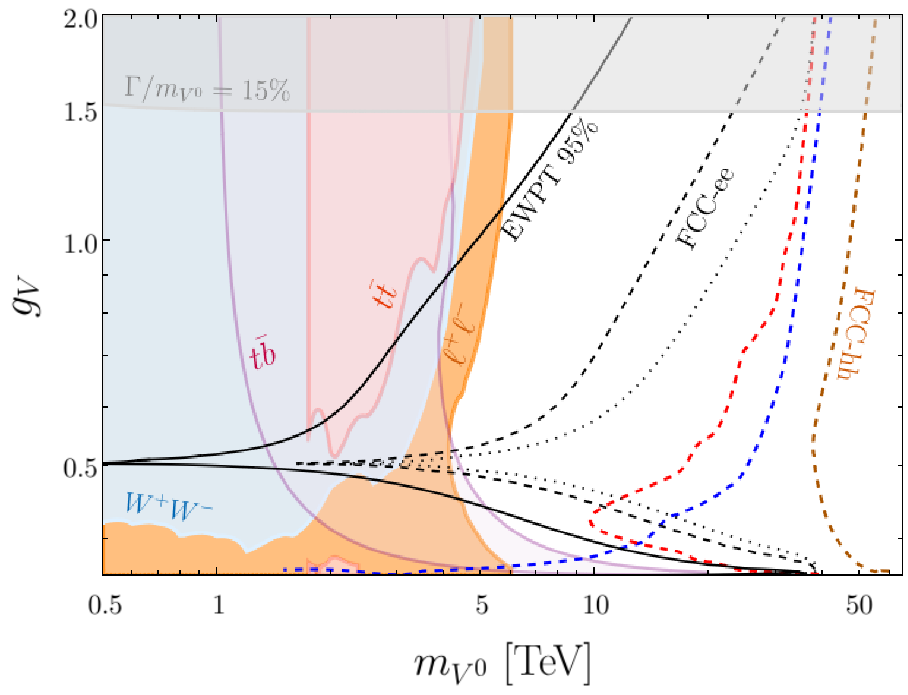

- Mass reach of 40–50 TeV in FCC-hh di-lepton channel
- EWPTs and direct searches exclude similar regions of parameter space
- FCC-hh nicely complements regions that EWPTs cannot exclude

Comparing limits for explicit models

<u>Model</u>:

Composite Higgs (strongly coupled)

- Up to 50 TeV reach at FCC-hh
- EWPTs better for large (and very small) values of g_V, especially for current LHC searches
- Combining searches ensures that most of the remaining parameter space is covered

FCC-ee: [1608.01509](1608.01509)

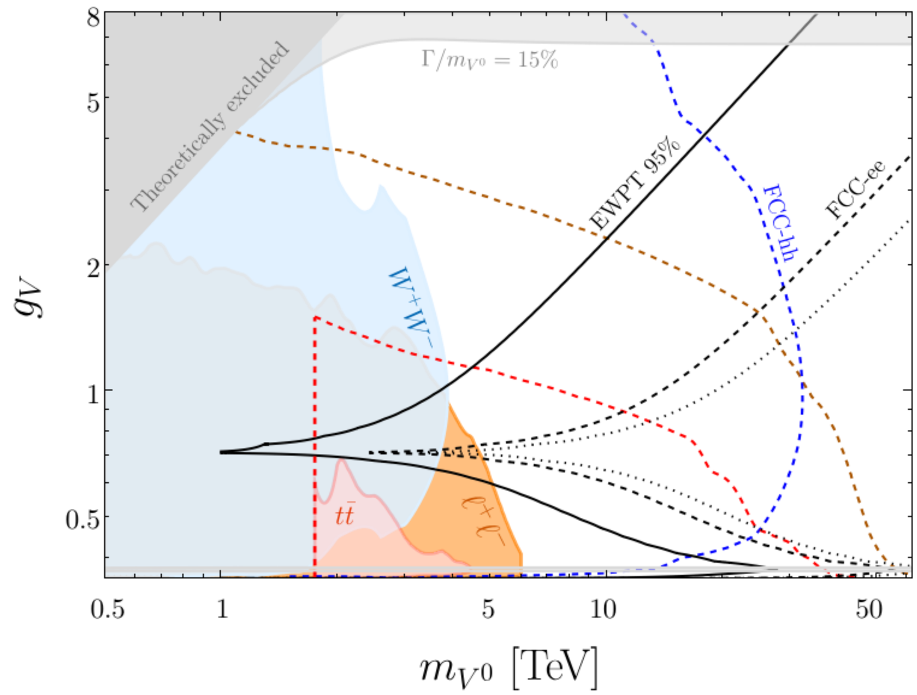

Summary

Using a simplified model of heavy vector singlets, we have motivated future efforts at colliders, highlighting the complementary interplay between indirect and direct searches.

- Of all currently proposed future colliders, the FCC-hh is best positioned to probe the multi-TeV region
- Prior to the hadronic phase, indirect hints at BSM physics provide by FCC-ee precision tests will motivate future direct searches
- The FCC-ee and FCC-hh complement each other – some regions of parameter space favour indirect versus direct searches, with FCC-hh able to explore the regions that EWPTs cannot

Extrapolation procedure

The upper limit on the number of signal events in a small window around the resonance mass depends exclusively on the the number of background events.

Equate the number of background events across the two colliders to obtain the "equivalent" mass, m, at the future collider:

$$\boxed{c_{ij} = \lim_{\hat{s}\to\infty} [\hat{s}\hat{\sigma}_{ij}(\hat{s})]}$$

$$B(s_0, L_0, m_0) = B(s, L, m) \longrightarrow \sum_{\{i,j\}} c_{ij} \frac{d\mathcal{L}_{ij}}{d\hat{s}}(m; \sqrt{s}) = \frac{L_0}{L} \sum_{\{i,j\}} c_{ij} \frac{d\mathcal{L}_{ij}}{d\hat{s}}(m_0; \sqrt{s_0})$$

The number of background events should be the same for a heavy vector of mass m as at the LHC for a mass m_0. We can re-scale the old cross-section by the ratio of the luminosities:

$$[\sigma \times \mathrm{BR}](m; s, L, L') = \frac{L_0}{\sqrt{LL'}} \mathrm{limit}[\sigma \times \mathrm{BR}]_0(m_0; s_0, L_0)$$

where we vary L' over the range L' ≤ L. The limit is then given by the minimum at each mass point over the range of L':

$$\mathrm{limit}[\sigma \times \mathrm{BR}](m; s, L) = \min_{L' \leq L} [\sigma \times \mathrm{BR}](m; s, L, L')$$

Explicit model branching ratios

We can produce similar branching ratio plots for the explicit models we consider:

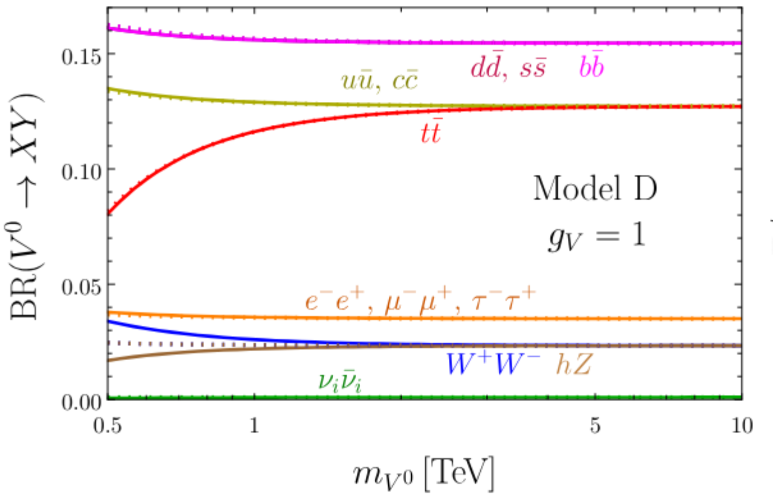

Model D: $SU(2)_L \times SU(2)_R \times U(1)_X$

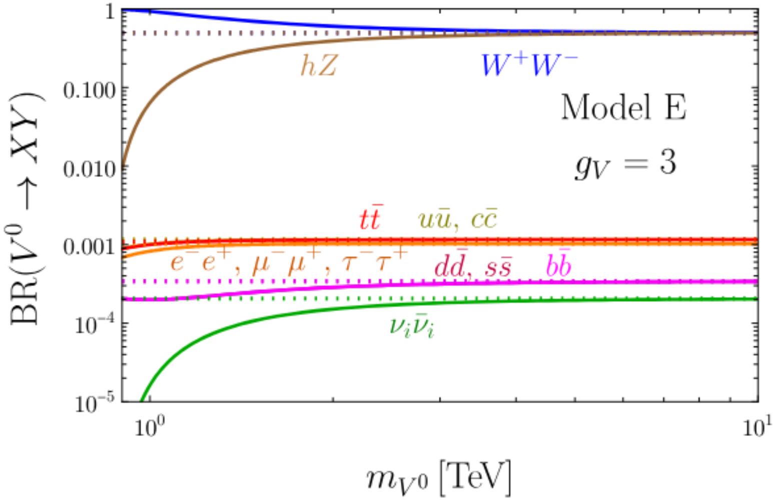

Model E: Composite Higgs

All future collider projections

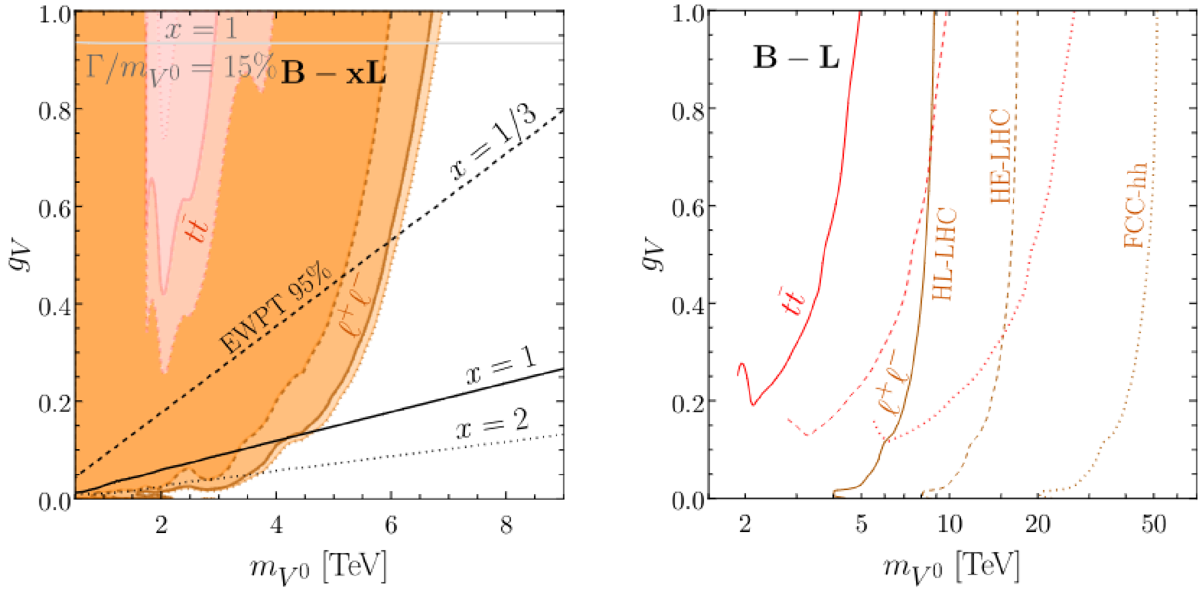

B – L symmetry

All future collider projections

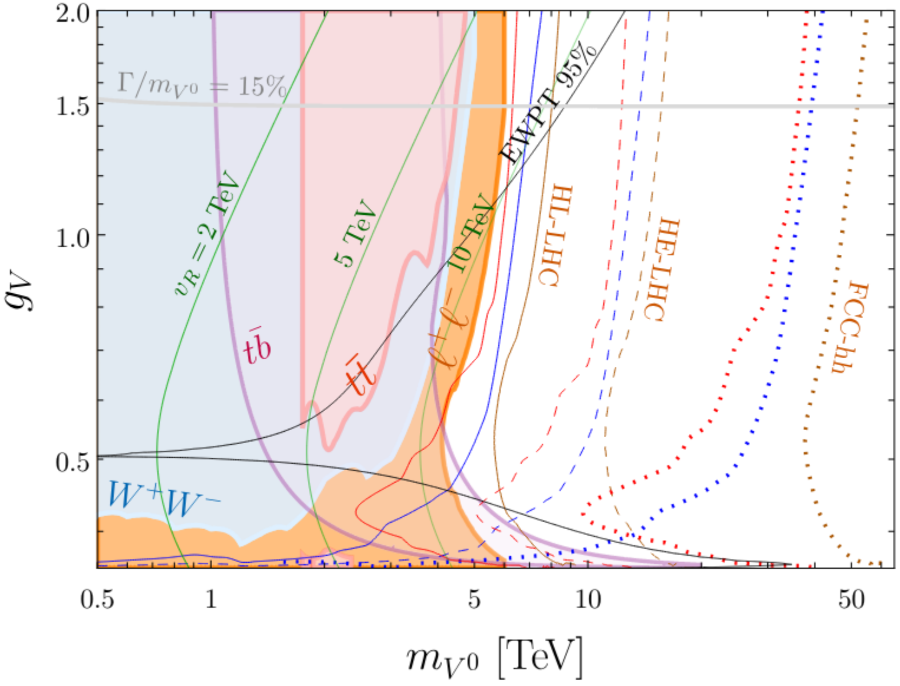

Model D: $SU(2)_L \times SU(2)_R \times U(1)_X$

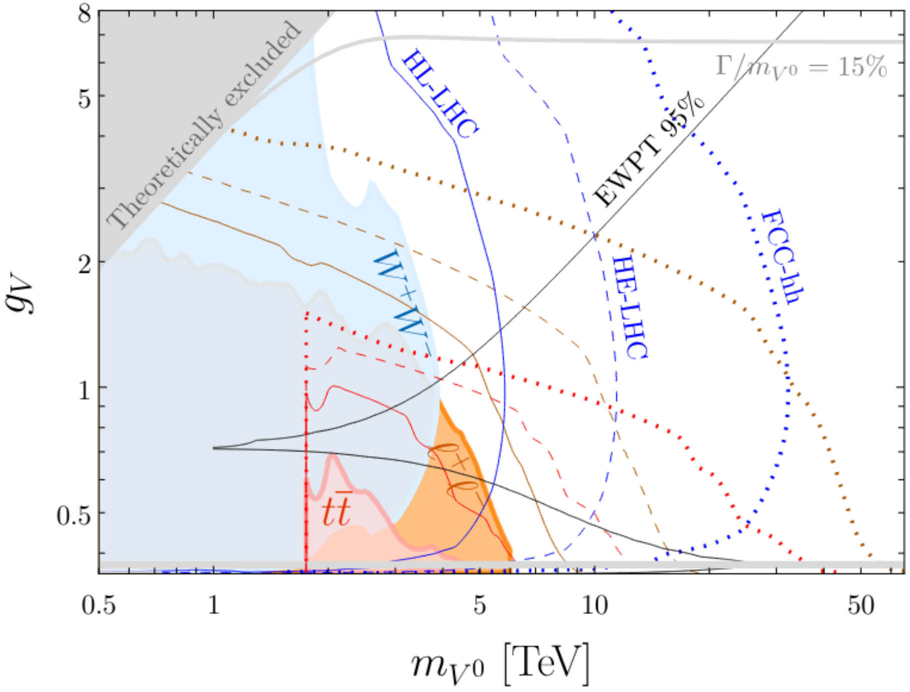

Model E: Composite Higgs